Electronic Supplementary Material (ESI) for Analyst.

<u>Supplementary Information</u>

A novel fluorescence method for the rapid detection of *Listeria monocytogenes* using aptamer-conjugated magnetic nanoparticles and aggregation-induced emission dots

Yuanyuan Guo,[a,#] Chao Zhao, [a,#] Yushen Liu, [a] Heran Nie, [b,*] Xiaoxiao Guo,[a] Xiuling Song,[a] Kun Xu,[a] Juan Li,[a] and Juan Wang [a,*]

[a] School of Public Health, Jilin University, Changchun, Jilin, 130021, PR China

[b] Dalian Institute of Chemical Physics, Chinese Academy of Sciences, Dalian, Liaoning, 116023, PR China

[#] These authors contributed equally to this work.

* Corresponding Author: li_juan@jlu.edu.cn; jwang0723@jlu.edu.cn

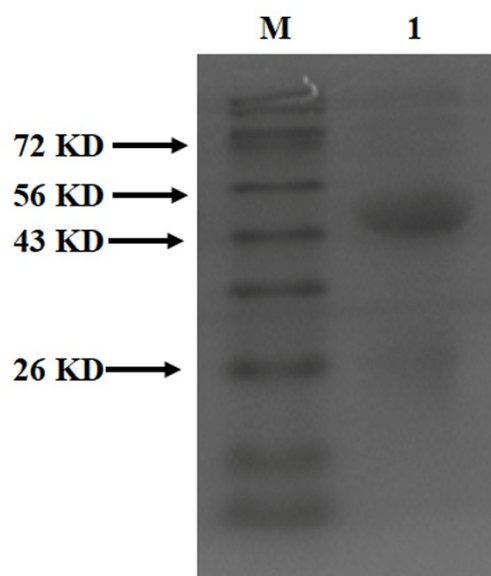## 1. SDS-PAGE result of rabbit IgG antibody of *L. monocytogenes*

Fig. S1 SDS-PAGE result of rabbit IgG antibody of *L. monocytogenes*. Protein marker (lane M); rabbit IgG antibody of *L. monocytogenes* (lane 1).

2. Synthesis and characterization of apt-MNP

The MNPs were prepared through a solvothermal method according to our previous paper [1], and apt-MNP was fabricated according to our previous literature [2]. In Fig. S2A, the TEM image shows apt-MNPs were well dispersed roughly spherical nanoparticles. And Fig. S2B shows the apt-MNPs captured *L. monocytogenes* closely. The FTIR spectrum of Fe_3O_4 MNPs (black curve) and apt-MNP (red curve) are demonstrated in Fig. S2C. The obvious characteristic band of Fe_3O_4 MNPs at 582 cm^{-1} and 3431 cm^{-1} can be attributed to the stretching vibration of Fe-O and O-H vibrations [3-5]. In comparison with Fe_3O_4 NPs, several new characteristic peaks were observed from the spectrum of apt−MNPs. Especially, the band at 1521 cm^{-1}, 1629 cm^{-1}, 2800 cm^{-1} and 2879 cm^{-1}, which are assigned to C=O bond, C=C bond, CH_2 groups, respectively [6]. Owing to the negative charge of the phosphate moieties of aptamer, the zeta potential of apt-MNP is sharply decreased from -68.45 to -90.87 mV (Fig. S2D). All these results confirm that the apt-MNP was expected to be synthesized as the aptamer of *L. monocytogenes* binds to MNP successfully.
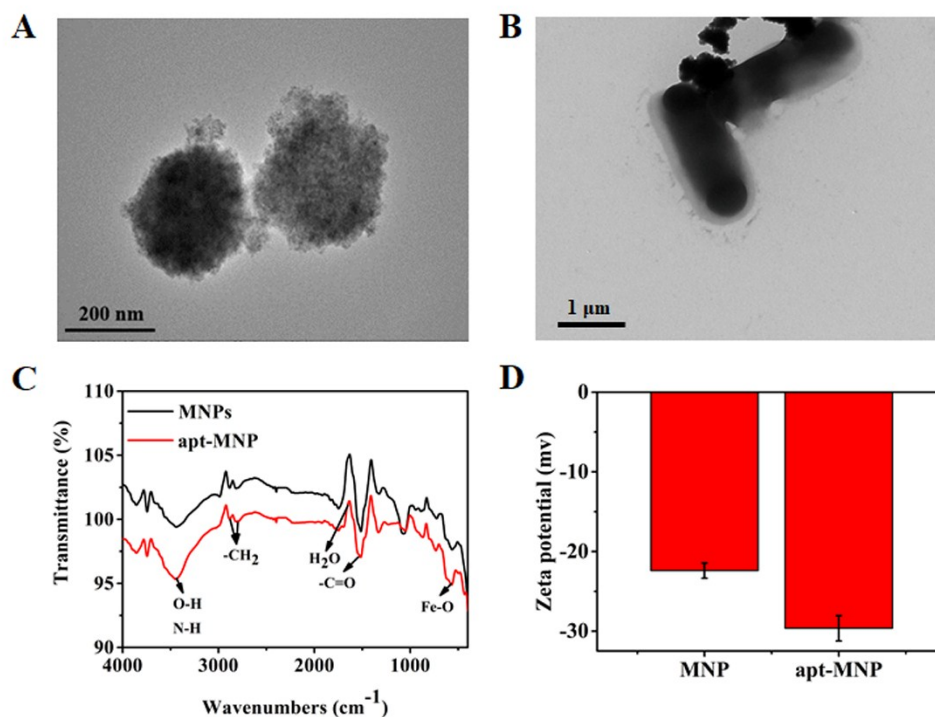
Fig. S2 (A) TEM images of apt-MNPs and (B) apt-MNP captured *L. monocytogenes*. (C) FT-IR spectrum of Fe_3O_4 MNPs and apt-MNP. (D) Zeta potential measurements of Fe_3O_4 MNPs and apt-MNPs.

3. The loading efficiency of TPE-OH@BSA NPs

The loading efficiency was measured by conducting three replicate analyses through a fluorescence spectrophotometer. The loading efficiency is expressed by $\Delta F/F_0$ ($\Delta F = F_0 - F$, where F_0 is the original fluorescence intensity of TPE-OH in THF/H_2O_2, and F is the fluorescence intensity of TPE-OH in the supernatant after encapsulated).

Table S1 The loading efficiency of TPE-OH@BSA NPs

Sample	F_0	F	Loading efficiency (%)	RSD (%)
1	4866.12	554.25	88.61	
2	4860.85	635.80	86.92	1.29
3	4872.63	513.09	89.47	

4. Optimization of the incubation time

To obtain the best incubation time, the fluorescence intensity of the reaction system with *L. monocytogenes* concentrations of 10^6 cfu·mL^{-1} was measured at 30, 45, 60, 90 and 120 min, respectively. Then use an external magnetic field to separate immune complex. Subsequently, the fluorescence intensity of the supernatant at 464 nm was measured. The difference of fluorescence intensity between negative and positive was calculated under different incubation time. As shown in Fig. S3, with the extension of reaction time, the difference between negative and positive gradually increased, and reached the maximum fluorescence intensity at 90 min, and then gradually decreased. Therefore, 90 min was selected as the best reaction incubation time.
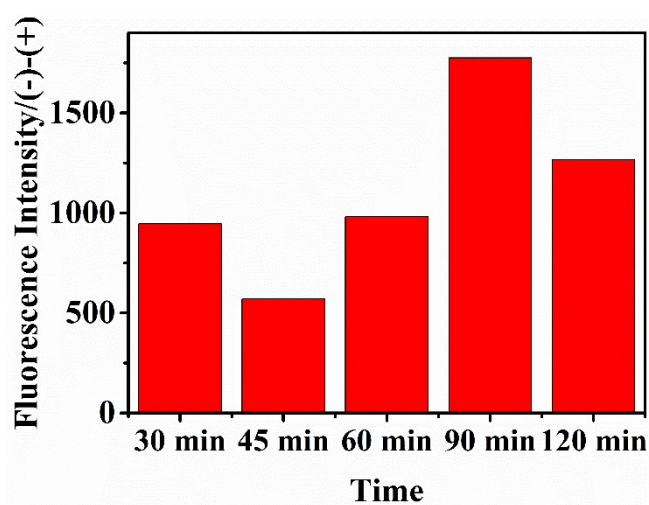

Fig. S3 Optimization of incubation time (30, 45, 60, 90, 120 min).

5. Detection of real samples

The calibration plot for *L. monocytogenes* in water from Nan Lake, Yan Lake and pork meat.
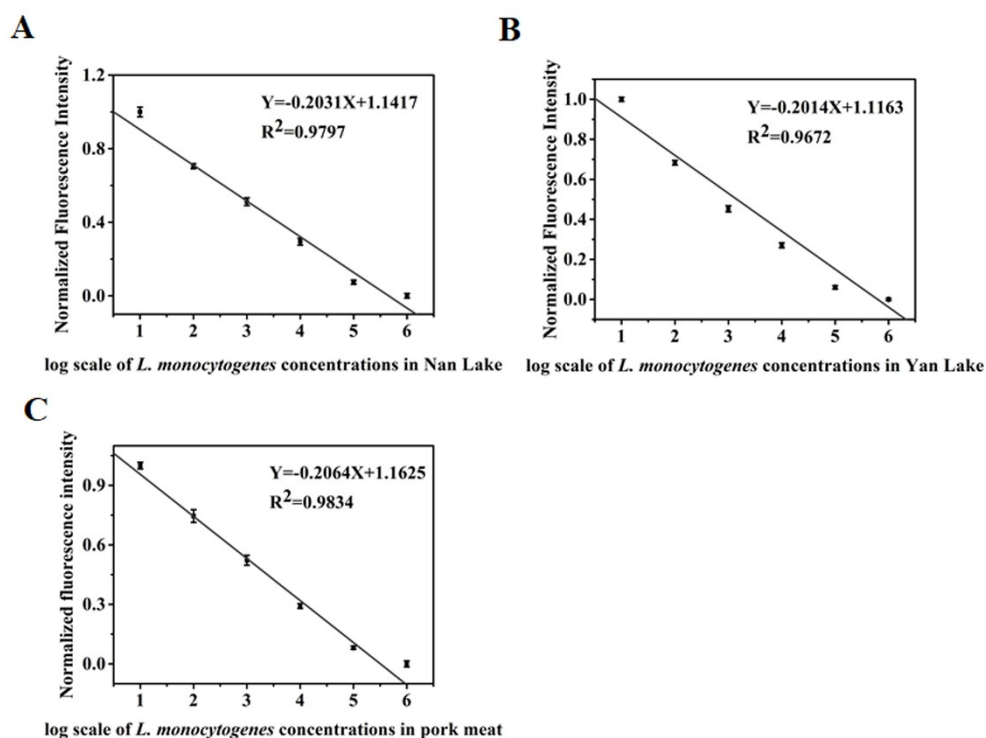
Fig. S4 (A) The calibration curve for *L. monocytogenes* in Nan Lake samples. (B) The calibration curve for *L. monocytogenes* in Yan Lake samples. (C) The calibration curve for *L. monocytogenes* in pork meat samples. (Fluorescence intensity vs the logarithm of *L. monocytogenes* concentration). Error bars represent the standard deviation of three replicates.

References

1 F. Kaiyue, Z. Yan, L. Juan, L. Yushen, P. Bo, S. Xiuling, X. Kun, W. Juan and Z. Chao, *Journal of Agricultural and Food Chemistry*, 2018, **66**, 9516-9521.

2 L. Yushen, W. Juan, S. Xiuling, X. Kun, C. Huisi, Z. Chao and L. Juan, *Microchimica Acta*, 2018, **185(8)**, 360.

3 G. Zhiqiang, S. Tingting, X. Jinfeng and F. Xuejiao, *Environmental Science and Pollution Research*, 2018, **26(3)**, 2387-2396.

4 Z. Dandan, G. Zhiyong, G. Pengfei, H. Xue, C. Xuwei and W. Jianhua, *ACS applied materials and interfaces*, 2018, **10**, 21876−21882.

5 Z. Zhide, W. Zhihong, Z. Le and L. Guiyin, *IOP Conference Series: Materials Science and Engineering*, 2018, **382**, 022035.

6 M. Eagambaram, J. J. Nimita, A. Mathivathanan, R. Saravanan, K. Janankiraman, C. R.

Akshata and K. Kalpana, *ACS Omega*, 2018, **3**, 13685-13693.